Martine Janet van de Weg, Patrick Meir, Mat Williams, Cécile Girardin, Yadvinder Malhi, Javier Silva-Espejo, John Grace

This article was accepted for publication in Ecosystems.

van de Weg, M.J., et al. 2014. Gross primary productivity of a high elevation tropical montane cloud forest. *Ecosystems*. 17(5): pp.751-764. Available from DOI: http://dx.doi.org/10.1007/s10021-014-9758-4

Running Head: Modeled GPP of a Peruvian montane cloud forest

Title: Gross Primary Productivity of a high elevation tropical montane cloud forest

Authors: Martine Janet van de Weg [1,2*], Patrick Meir[2, 3], Mat Williams[4], Cecile Girardin[5], Yadvinder Malhi[5], Javier Silva-Espejo[6] and John Grace[3]

[1] *Amsterdam Global Change Institute, Vrije Universiteit Amsterdam, De Boelenlaan 1085, 1081 HV, Amsterdam, The Netherlands*

[2]*School of Geosciences, University of Edinburgh, Drummond Street, Edinburgh EH8 9XP, UK*

[3] *Research School of Biology, Australian National University, Canberra, ACT 0200, Australia*[4]*School of Geosciences, University of Edinburgh, Crew Building, Edinburgh EH9 3JNB, UK*

[5] *Environmental Change Institute, School of Geography and the Environment, University of Oxford, South Parks Road, Oxford, OX1 3QY, UK*

[6]*Universidad San Antonio Abad del Cusco, Avenida de la Cultura No 73, Cusco, Peru*

[*]Corresponding author. Email: m.j.vande.weg@vu.nl

Abstract

For decades, the productivity of tropical montane cloud forests (TMCF) has been assumed to be lower than in tropical lowland forests due to nutrient limitation, lower temperatures and frequent cloud immersion, although actual estimates of gross primary productivity (GPP) are very scarce. Here we present the results of a process-based modeling estimate of GPP, using a Soil-Plant-Atmosphere model (SPA), of a high elevation Peruvian TMCF. The model was parameterized with field-measured physiological and structural vegetation variables, and driven with meteorological data from the site. Modeled transpiration corroborated well with measured sap flow, and simulated GPP added up to 16.2 ± SE 1.6 Mg C ha^{-1} yr^{-1}. Dry season GPP was significantly lower than wet season GPP, but this difference was 17% and not caused by drought stress. The strongest environmental controls on simulated GPP were variation of photosynthetic active radiation (PAR) and air temperature (T_{air}). Their relative importance likely varies with elevation and the local prevalence of cloud cover. Photosynthetic parameters (V_{cmax} and J_{max}) and leaf area index (LAI) were the most important non-environmental controls on GPP. We additionally compared the modeled results with a recent estimate of GPP of the same Peruvian TMCF derived by the summing of ecosystem respiration and net productivity terms, which added up to 26 Mg C ha^{-1} $year^{-1}$. Despite the uncertainties in modeling GPP we conclude that at this altitude GPP is, conservatively estimated, 30-40% lower than in lowland rainforest and this difference is driven mostly by cooler temperatures than changes in other parameters.

Keywords: SPA model, sap flow, diurnal photosynthesis, carbon fluxes, Peru, Andes, gross primary productivity (GPP), net primary productivity (NPP), autotrophic respiration, carbon expenditure

Introduction

Characterized by the frequent occurrence of clouds and mist and usually found between 1000 to 3000 m above sea level (a.s.l.), tropical montane cloud forests (TMCF) differ from lowland rainforests in both their structure and functioning. For example, the TMCF tree stature is smaller, their leaves have a higher leaf mass per area (LMA), and leaf area index (LAI) is lower (*e.g.* Grubb and Whitmore 1966, Tanner and others 1998, Kitayama and Aiba 2002, Moser and others 2007, van de Weg and others 2009). TMCFs net primary productivity (NPP) is also low compared with lowland rainforests, and productivity decreases with increasing altitude in rates ranging between 1.0-6.6 Mg C ha^{-1} yr^{-1} km^{-1} (Raich and others 1997, Kitayama and Aiba 2002, Girardin and others 2010). Explanations for the lower productivity of TMCFs include the lower levels of photosynthetic active radiation (PAR) because of frequent cloud immersion, lower average temperatures, periodic water deficiencies, leaf wetness that potentially inhibits photosynthesis, and lower nutrient supply (Bruijnzeel and Veneklaas 1998, Waide and others 1998, Letts and Mulligan 2005). The latter hypothesis has been tested by adding nutrients (nitrogen and phosphorus) to this ecosystem and in some cases, but not all, this resulted in increased TMCF stem growth and litter fall (*e.g.* Tanner and others 1990, Tanner and others 1992, Vitousek and Farrington 1997, Adamek and others 2009, Fisher and others 2012). However, the influence of environmental variables, such as the lower total incident PAR and lower temperatures, have not been tested experimentally, or through detailed process-based modeling. Nonetheless, both light and temperature have been regarded to be key environmental controls on TMCF productivity (Bruijnzeel and Veneklaas 1998).

Overall, estimates of TMCF gross primary productivity (GPP) are rare, probably also because observations of stand scale CO_2 fluxes with the eddy covariance technique are difficult

47 in the mountainous terrains of TMCFs (Kaimal and Finnigan 1994). However, contrasting with
48 the paradigm of decreasing productivity with increasing altitude, a recent calculation of the GPP
49 of an Andean TMCF at 3025 m a.s.l. resulted in estimates of 25.9 ±3.1 Mg C ha^{-1} yr-1(Girardin
50 and others 2013). This GPP value is only slightly lower than observed values from tropical
51 lowland Amazonian rainforests (*e.g.* Fisher and others 2007, Hutyra and others 2008; Malhi and
52 others 2009, Miller and others 2011), which range from 30-40 Mg C ha^{-1} $year^{-1}$. The GPP
53 estimate of 25.9 Mg C ha^{-1} yr-1was based on quantifying the carbon expenditure of the forest,
54 summing all the autotrophic respiration (R_a) and net primary productivity components of the
55 ecosystem (*e.g.* Ryan and others 2004). Other TMCF GPP estimates are based on modeling
56 exercises, although these studies are also scarce. Wang and others (2003) modeled annual GPP
57 values of 60.32 – 24.08 Mg C ha^{-1} yr^{-1} over an altitudinal range of 450-1050 m a.s.l. respectively
58 in the Luquillo mountains in Puerto Rico, using a canopy process model driven with simulated
59 climate data from a topographical climate model and remotely sensed LAI data derived from
60 NDVI measurements. However, for the high altitude sites this model overestimated GPP up to
61 40% compared with field observations. In addition, Marthews and others (2012) modeled the
62 GPP of a Peruvian TMCF with the land surface model JULES, but their simulation returned
63 values of only 1.25 Mg C ha^{-1} yr^{-1}, which was the result of the model not capturing TMCF
64 vegetation very well. In sum, there are still very few estimates of GPP in TMCF, and
65 consequently, questions regarding the environmental controls on GPP in TMCF remain open.

66 In this study we simulated the GPP of a TMCF at 3025 m a.s.l. in Peru with the process
67 based Soil-Plant-Atmosphere (SPA) model developed by Williams and others (1996, 2001a).
68 The SPA model has performed well in simulating a wide range of ecosystems (Williams and
69 others 1996, Williams and others 2001a and 2001b, Wright and others 2013) and simulated the C

and H_2O fluxes of an Amazonian lowland rainforest particularly well when the model output was evaluated against stomatal conductance, sap flow and eddy covariance measurements (Fisher and others 2006, Fisher and others 2007, Fisher and others 2008). For our study we parameterized the model with data collected by ourselves and others, from the same site investigated by Girardin and others (2013). We used *in situ* measured leaf photosynthetic parameters and leaf traits, canopy, root and soil structure data, and the model was driven with a year of weather data recorded at the same site. Validation of the model's performance was done by comparing it with *in situ* collected sap flow data, and simulated leaf level photosynthesis of the upper canopy layer with some *in situ* measurements. We investigated how TMCF GPP is controlled by environmental conditions and canopy structure, as informed by analyses of SPA (Fisher and others 2007, Fox and others 2009). The hypotheses we tested were: 1) TMCF GPP is lower than observed in tropical lowland forests. 2) The key environmental determinants of lower TMCF GPP are temperature and PAR, while water deficiencies are of little importance under the current climate. 3) GPP varies little throughout the seasons, as temperature and PAR are expected not to change substantially throughout the season. In addition, we discuss the discrepancies between our process based modeled results and the GPP estimates of Girardin and others (2013) made by summing growth and autotrophic respiration terms.

Methods

Research site

The TMCF that we simulated with the SPA model is a one-ha plot in the Kosñipata valley in Peru at 3025 m a.s.l. (13º11'28''S / 71º35'24''W). The plot is located in the cultural buffer zone of the Parque Nacional del Manú, Cusco, near the Wayquecha research station. The vegetation is a closed canopy forest with a relatively low mean canopy height 12.8 ± SE 0.46 m (n=180),

while average soil depth is 0.44 ± SE 0.06 m (n =20). Average annual air temperature (T_{air}) is 12.5 ºC, and annual rainfall ranges between 1700 and 2000 mm yr^{-1}. The forest is dominated by species in the *Weinmannia* and *Clusia* genera that together represent 56% of the number of trees in the plot, with *Weinmannia crassifolia* being the most dominant of species (~35% of individual trees).

Meteorology

An automated weather station (Campbell Scientific Ltd, UK) collected and stored meteorological data using a data logger (CR3000, Campbell Scientific Ltd, UK). Precipitation was measured with a tipping bucket rainfall gauge, together with two fog collectors (harp and mesh), all three with a 0.2 mm resolution (Campbell Scientific Ltd, UK). PAR was measured with a PAR quantum sensor (Skye Instruments Ltd, Powys, UK), while a net radiometer measured short wave radiation (SWR) (CNR1, Kipp & Zonen, Delft, Netherlands) and the diffuse radiation was registered with a sunshine sensor (BF3, Delta-T Devices Ltd, Cambridge, UK). T_{air} and relative humidity were measured with a combined HMT sensor (Vaisala, Oy, Finland), and vapor pressure deficit (VPD) was automatically calculated from those data. Wind speed measurements were failed for this period, except for 9 days, so average wind speed in the model was set at 1.0 m s^{-1}. Other meteorological data were missing from 27 February 2009 to 3 March 2009 and for 30 April 2009. Data for these two gaps were filled with mean monthly diurnal values. For SWR, data were missing from 19 September 2008 to 9 December 2008, representing 22% of the SWR dataset. These gaps were filled by recalculating the SWR from the collected PAR data in that period, using a regression from the available PAR and SWR data

Sap flux

To validate the results of the SPA model we used sap flow rates, measured on 12 trees in the research plot. The species included were *Clusia cretosa* (Hammel ined.) (5 trees), *Weinmannia crassifolia* (3 trees), *Prunus integrifolia* (1 tree) *Clusia flavifora* (1 tree) *Weinmannia bangii* (1 tree) and a *Clethra* species not identified to species level (1 tree). Sap flow sensors were installed in April-May 2007 on trees that represented the diameter at breast height (DBH) distribution present in the plot (12.9-38.1 cm). Measurements were made using the trunk segment heat balance method described by Čermák and others (1973, 2004) (Sap Flux Meter P4.1, Environmental Measuring Systems, Brno, Czech Republic). Limited power supply throughout the year restricted data collection period between 16 July 2008 to 1 September 2008, with five days missing because of power failure. Because the sap flow rates per sapwood area (J, g m^{-2} s^{-1}) were proportional to the basal areas of the measured trees, plot level sap flow could consequently be scaled with the plot basal area.

Photosynthesis and water potential measurements

The Rubisco carboxylation efficiency (V_{cmax}) and electron transport efficiency (J_{max}), which are the photosynthetic parameters needed for the model, were derived from A-C_i curves measured on *Weinmannia crassifolia, Clethra cuneata*, *Schefflera allocotantha*, *Prunus integrifolia*, and *Clusia creatosa*. We used portable photosynthesis equipment fitted with an LED light source (a Li-Cor 6400with a 6400-02B Red/Blue Light Source, Li-Cor, Lincoln Inc,) and the A-C_i curves were performed at an average temperature of 20.4°C (±SE 0.3 °C) since observed *in situ* mid-day leaf temperatures ranged between 15-25°C. A detailed description of the A-Ci curves and curve-fitting routine is found in supplementary information I and in Van de

Weg and others (2012). The average V_{cmax} and J_{max} per canopy layer in the model were consequently based on the (proportional) basal area per species and their estimated presence per canopy layer (Table 1 and Supplementary Information I).

In order to validate the modeled foliar photosynthesis rates (A_{net}) and the leaf temperatures (T_{leaf}), *in situ* data for A_{net} and T_{leaf} were collected on individuals next to the research plot and that were fully sun-lit and accessible from the ground to guarantee an intact water column. For A_{net}, fully sunlit, non-damaged leaves of *Weinmannia crassifolia*, *Clethra cuneata*, *Schefflera allocotantha*, and *Clusia cretosa* were measured on 14, 24 and 28 August 2008 at between 06:00 and 17:00 on one or two leaves from three individual trees per species. The light source of the LI-6400 was set in the mode to follow the ambient PAR observed by the external quantum sensor of the Li-Cor 6400 head. This setting was preferred over using leaf chamber with transparent top, to avoid shading of the 6 cm^2 leaf area in the cuvette, caused by the cuvette frame under certain angels of ambient illumination. T_{leaf} measurements were derived from these photosynthesis measurements and from a dataset collected with a portable dynamic diffusion porometer (Delta-T AP4, Delta-T Devices Ltd, Cambridge, UK), which is equipped with a leaf-contact thermocouple. In total, T_{leaf} was measured on five individuals for the same species on three sunlit leaves between 6:00 and 17:00 on 19, 21, 23 and 28 July and 14, 24 and 28 August 2008.

On the same days as the T_{leaf} measurements, minimum leaf water potential (Ψ_{leaf}) was measured at with a pressure chamber (Skye Instruments Ltd, Powys, UK) on the same four species to obtain the minimum Ψ_{leaf} to parameterize the SPA model with.

Structural vegetation and soil characteristics

The gap fraction of the canopy using a hand-held spherical densiometer (Lemmon 1956), we derived the leaf area index (LAI) in July 2008 at 180 locations equally distributed in the 1 ha research plot, in order to get a large spatial coverage plot LAI. Average dry season LAI was similar to dry season values from Girardin and others (2013), being 4.2 ± 0.04 and 4.1 ± 0.15, respectively. Monthly changes in LAI throughout the year were then based on the variability provided by Girardin and others (2013), who used the hemispherical photographic method on 25 locations in the research plot. The fraction LAI per canopy layer (top-middle-canopy) was estimated visually from the trees from which V_{cmax} and J_{max} values had been measured (n =25). Root biomass, root density and root biomass density values were taken from Girardin and others (2010) and rooting depth of fine roots was up to 30 cm. Soil properties (organic fraction, sand and clay fraction of the soil) were adapted from Zimmermann and others (2009) and soil porosity was calculated according to Saxton and others (1986).

Modeling methodology

A detailed description of the SPA model (v. 1) is found in Williams and others (1996, 2001a). The model runs at 30-minute time steps and explicitly simulates the radiative transfer of direct and diffuse PAR through 10 separate canopy layers. Foliar C-uptake is based on the Farquhar equation for C_3 photosynthesis (Farquhar and others 1980) and the Penman-Monteith equation determines leaf-level transpiration. These two processes are linked by a model of stomatal conductance that optimizes daily C gain, while maintaining Ψ_{leaf} above the threshold value. Maximum stomatal conductance (g_s) was set at 0.5 mol m^{-2} s^{-1}, which approximates maximum observed g_s. Iota (ι, dimensionless), the parameter that determines the minimal

185 increase in photosynthesis necessary for stomata to open, was set at 1.0007 (*i.e.* g_s is incremented
186 until C-uptake no longer increases by more than 1-ι, as long as minimum Ψ_{leaf} is not crossed).
187 Furthermore, the temperature response curves of the photosynthetic parameters V_{cmax} and J_{max} are
188 fitted to the polynomial relationships found in McMurtrie and others (1992).
189 The SPA model also couples canopy transpiration with hydraulic transport from the root
190 system, simulating hourly and daily sap flow directly. The inclusion of a capacitance term in the
191 hydraulic model generates a time lag between leaf losses and stem transport of water, and was
192 set to 5000 mmol MPa^{-1} m^{-2}, which matched the tails of *in situ* hourly sap flow during each
193 evening. The hydraulic conductivities (*i.e.* stem conductivity and root resistivity) were calibrated
194 with leaf specific conductance (LSC, mmol m^{-2} s^{-1} MPa^{-1}), assuming aboveground and
195 belowground hydraulic resistance to be approximately equal (Table 2). LSC was calculated with
196 independent transpiration measurements (E, mmol m^{-2} s^{-1}) and Ψ_{leaf} measurements made from 2-
197 5 August 2008 on four species that were selected for A_{net} measurements, assuming:
198 $\Delta\Psi = \Psi_{leaf} - \Psi_{predawn}$
199 and
200 $LSC = E/\Delta\Psi$
201 A detailed list of the model parameters and how they were retrieved can be found in
202 Supplementary Information II.
203

204 *Sensitivity analyses*

205 Sensitivity analyses were performed for most of the model's parameters and
206 environmental drivers in order to investigate which are the most important factors that control
207 GPP in the SPA-simulated TMCF, given their range of observed values in the field (Table 3). In

addition to the providing absolute changes in GPP per changed parameter (ΔGPP), we determined their relative importance by dividing the proportional increase in parameter from minimum to maximum by the proportional increase or decrease in simulated GPP. Each factor was changed individually, keeping daily and seasonal variation proportional to the original observed values, while also keeping other drivers and parameters as in the original simulation. The sensitivity analyses for changes in V_{cmax} and J_{max} were conducted simultaneously since they vary in proportion with each other (Wullschleger 1993, Meir and others 2002). This simultaneous variation was also done for changes in PAR and SWR. Field measurements of capacitance and ι were not available, so we tested the sensitivity to changes of capacitance between 3000 and 7000 MPa^{-1} m^{-2}, and for ι between 0.001 and 0.0001.

In addition, with three factors from the sensitivity test that explained a large part of the variation in the TMCF GPP (T_{air}, PAR and LAI), additional simulations were performed to estimate TMCF GPP under tropical lowland forests conditions. Again, temporal variation in the environmental drivers and LAI were kept proportional to the original observed values. The maximum values for the drivers T_{air} and PAR, and the structural parameter LAI, did not originate from one particular tropical lowland site, but were set to rounded values within the range of values obtained from the literature (*e.g.* Domingues and others 2005, Fisher and others 2007, Malhi and others 2009) (Table 4).

Results

Meteorology and environmental drivers

Precipitation was the strongest seasonal pattern in the meteorological drivers (Figure 1). The warmest month coincided with the wettest period, in November 2008 (11.2 ºC ± SD 1.1),

while the coldest month was in the 'dry' season in June 2009 (9.9 ºC ± SD 1.0). April 2009 had the lowest mean average PAR (based on 24 hrs averages) (18 mol m^{-2} d^{-1}± SD 8) and September 2008 the highest (25 mol m^{-2} d^{-1} ± SD 17) (Fig. 1b). Maximum daily VPD did not exceed 1.31 kPa, while the average daily VPD was 0.52 kPa. Even throughout the dry months May-September (average VPD was 0.21 kPa) days with very low VPD values (< 0.007 kPa) occurred (Figure 1c).

Modeled sap flux and modeled GPP

The model simulated the hourly sap flow well, both for the values (R^2= 0.87, root mean square error of approximation (RMSE) =0.021 mm hr^{-1}) and for the diurnal patterns (Figure 2.). Daily sap flow is somewhat underestimated by the model (Figure 2a), but there was no systematic bias for days with either large or small transpiration values. Modeled transpiration was 223 mm y^{-1} and total estimated annual GPP at 16.2 Mg C ha^{-1} yr^{-1} (Figure 3a). Daily transpiration varied between 0.03 - 2.0 mm day^{-1}, while GPP varied from 1.91– 6.87 g C m^{-2} day^{-1}. Total transpiration and GPP varied throughout the year (Figure 3a), with daily GPP being significantly lower (P<0.001, Student's t-test) in the dry season month June (39.9 kg C ha^{-1} day^{-1})compared with wet season month October (47.9 kg C ha^{-1} day^{-1}). For the these months PAR and T_{air} were significantly different as well, with daily PAR being 18 mol m^{-2} d^{-1} *vs.* 23 mol m^{-2} d^{-1} (P<0.002) and T_{air} 9.9 °C *vs.* 10.7 °C (P<0.002), for June and October respectively. Modeled transpiration being was in December (0.37 ± 0.08 mm day^{-1}) when average VPD was lowest (0.33 ± 0.04) kPa.

Modeled and measured leaf level photosynthesis and leaf temperature

254 The A_{net} and T_{leaf} measurements were not done continuously and not for all species on the
255 same days, hindering a 1:1 comparison with the canopy-scale modeled output. Almost all the
256 day-time measured *in situ* T_{leaf} values between 8:00 and 17:00 were higher than the modeled
257 average $T_{leaf,}$ from the upper canopy layer (layer 1 out of 10) (on average 3.25 °C higher).
258 Similarly, modeled maximum A_{net} of the fully sunlit leaves from the top canopy layer was lower
259 than for some of the *in situ* A_{net} measurements, especially for *S. allocotantha* and *C. cuneata*
260 (Figure 4c and 4d), although average modeled A_{net} resembles the A_{net} pattern from *W. crassifolia*
261 leaves (Figure 4c and 4d).
262

263 *Sensitivity analyses*

264 In absolute terms, using the range in daily observed PAR values caused the largest ΔGPP
265 (Table 3, figure 5c), increasing GPP with 14.7 Mg C ha^{-1} yr^{-1}. However, if we look at what
266 environmental parameter caused the largest relative change in GPP per relative parameter
267 change, GPP was more sensitive to daily temperature (Table 3). Similarly for the vegetation
268 parameters, absolute GPP values were most sensitive to changes in V_{cmax} and J_{max} (Table 3,
269 Figure 5a). For relative sensitivity, however, LAI (with N in leaves staying constant) was the
270 most important structural parameter (Table 3, Figure 5b). In contrast, GPP was insensitive to
271 changes in environmental drivers or model parameters that were involved in the site's hydrology.
272 For example, GPP was insensitive to changes in the range of observed mean daily VPD (Table 3,
273 Figure 5d) and no effects on simulated GPP were found when changing capacitance, ι, root
274 biomass and aboveground or belowground resistivity (Table 3). In fact, if we wanted to reduce
275 simulated GPP by 1% through changes in plant resistivity, plant hydraulic conductance needed to
276 be reduced to 0.2 mmol m^{-1} s^{-1} MPa^{-1}, which is a reduction of more than 90% from the minimum

observed in the field (Table 3). Likewise, SWC had to be decreased to 0.1 (a value not observed in the dataset), in order to simulate any reduction in GPP.

Finally, changing some drivers and parameters to values found in lowland tropical forests showed that increasing T_{air} increased modeled TMCF GPP by around 30% (Table 4). Increasing the PAR and LAI values increased GPP too, though less substantially (by 17% and 15% respectively), while increasing all three factors simultaneously increased GPP by almost 75%.

Discussion

Simulating transpiration

Only a daily basis, modeled sapflow was a little lower though than observed daily sap flow, but for daily sap fluxes the modeled values were consistent in their onset, peak and ending compared to the observed patterns (Fig 2). This consistency with independent stomatal behavior data was also observed by earlier uses of the SPA model in tropical forests (*e.g.* Fisher and others 2006, 2007). This suggests the model simulates diurnal stomatal activity sufficiently well to simulate stand scale water use within the range of meteorological drivers measured at our site. Our modeled transpiration rate of 223 mm $yr^{-1}$is slightly lower than the estimate of 250-300 mm from Bruijnzeel and Veneklaas (1998) but, consistent with these authors, much lower than values reported for tropical lowland rain forests (1000-2000 mm, Fisher and others 2010). Furthermore, simulated daily transpiration (up to 2.05 mm day^{-1}, average of 0.61 mm day^{-1}, Fig 3b) was comparable with ranges reported for TMCFs in Hawaii and Panama (0.39-1.02 mm day^{-1}, Zotz and others 1998, Santiago and others 2000), and similar to these forests, our sap flow measurements do not show midday stomatal closure (Fig 2b). The low TMCF transpiration rates are likely attributed to the low VPD values (*i.e.* low atmospheric demand). Together with the

300 insensitivity in transpiration at this site to changes in plant or soil hydraulic parameters and
301 drivers (*e.g.* root resistivity, plant conductance, Table 2) our analysis implies that a negative
302 water balance in this forest is an unlikely scenario under current climatic conditions.
303
304 *Simulating GPP*
305 In contrast with the transpiration, validating modeled GPP at high temporal resolution is difficult
306 since GPP can only be calculated, even when eddy covariance data are available, which they are
307 not for this environment. At first sight, our GPP estimate of 16.2 Mg C ha^{-1} yr^{-1} fits with the
308 paradigm that GPP in tropical montane cloud forests (TMCF) is substantially lower than that of
309 lowland tropical rain forests, since GPP values for the latter ecosystems vary between 30 - 40
310 Mg C ha^{-1} yr^{-1} for Amazonian and Asian rainforests (*e.g.* Hutyra and others 2008; Malhi and
311 others 2009, Hirata and others 2008). If we assume that the SPA model captures the C-fluxes as
312 well as the H_2O fluxes, the modeled GPP supports our hypothesis (H1) that TMCF GPP is lower
313 than the GPP of tropical lowland forests. Furthermore, extending the sensitivity analysis to
314 represent a lowland-upland climate contrast, the increased ranges in T_{air} and PAR associated with
315 this contrast (Table 4) support the second hypothesis (H2) that T_{air} is the most important factor
316 controlling TMCF GPP over this elevation difference (~ 3000 m). PAR is the second most
317 important environmental control over this elevation difference, although it was most important in
318 absolute terms for determining the natural variation in GPP at our site (Fig 5c). For a long time,
319 both lower temperatures and PAR levels have been hypothesized to be important in limiting
320 TMCF growth (Bruijnzeel and Veneklaas 1998, Waide and others 1998). Our analysis quantifies
321 the relationship rigorously and enables an interpretation of their absolute and relative importance
322 the researched altitude. Changes in soil water content or VPD within the range of observed

values were of little importance under the current climate in the 3025 m a.s.l. TMCF, as they did not constrain modeled canopy gas exchange. The 17% difference in modeled GPP between the wet and dry season months October and June was a significant difference, contrary to what we hypothesized (H3). This difference is unlikely to be caused by actual drought stress (despite the term 'dry season'), given the insensitivity of the modeled forest to changes in the hydrological drivers and parameters (Table 3). It is most probably that the lower daily PAR and daily T_{air} in June *vs.* October (18 mol m^{-2} d^{-1} *vs.* 23 mol m^{-2} d^{-1}, and 9.9 °C *vs.* 10.7 °C, respectively) that are the cause of this difference.

For the structural and biochemical parameters of the model, GPP was most sensitive to changing the photosynthetic parameters V_{cmax} and J_{max} , and LAI (Fig, 4a and c), and insensitive to changes in the belowground structural parameters (Table 3). The latter might be because the simulated TMCF did not experience any high VPD values (as also supported by the sap flow data). The sensitivity of GPP to increases in V_{cmax} and J_{max} or LAI is consistent with the hypothesis that TMCF productivity is N-limited (Tanner and others 1998) if it is assumed that higher N availability would lead to more N investment in more leaves for photosynthesis of higher investments in photosynthetic apparatus per leaf. However, both might not happen in reality, since fertilization experiments in TMCFs have shown that N addition does not always lead to increases in foliar N concentrations, or LAI (Tanner and others 1992, Fisher and others 2012). Furthermore, although the V_{cmax}-N relationship observed in this TMCF is significant, it contained notable between-species variance (van de Weg and others 2012). Nonetheless, irrespective of issues of N-limitation in TMCFs, the high absolute sensitivity of GPP to V_{cmax} and J_{max} emphasize the importance of estimating these parameters accurately when modeling GPP.

346

347 *Validation of the GPP estimate*

348 When we compare our GPP results with the modeled result from an altitudinal range of
349 450-1050 m a.s.l. in the Luquillo mountains in Puerto Rico (Wang and others 2003), which was
350 60.3 – 24.1 Mg C ha^{-1} yr^{-1}, our GPP estimate is low. However, the model from Wang and others
351 (2003) overestimated the high altitude GPP by 40% compared with field observations. This
352 overestimation can be partially explained by the retrieval of their model parameters, as this was
353 done remotely (*i.e.* no site-derived parameters in the model). Furthermore, the average LAI
354 values of their simulated transect were substantially overestimated (Wang and others 2003). In
355 contrast, our results were based on detailed site-measured vegetation parameters and
356 meteorological drivers. Overall, we find therefore it unlikely that our results represent a
357 substantial underestimation compared to the results from Wang and others (2003).

358

359 Another TMCF GPP quantification, from the same 3025 m a.s.l. TMCF in Peru, was
360 based on the carbon expenditure of the forest (*i.e.* the sum of all measured NPP and autotrophic
361 respiration ($R_{a)}$ terms) (Girardin and others 2013). At 25.9 ± 3.1 Mg C ha^{-1} yr^{-1}, this was 60%
362 higher than our process-model based estimated of GPP, which is substantially larger than the
363 intrinsic error for the SPA model of 10% (Fox and others 2010). Below we consider some factors
364 that might explain this mismatch between the GPP estimates.

365 First, although SPA adequately simulated stomatal behavior, GPP could be
366 underestimated if A_{net} was underestimated. The two species *C. cuneata* and *S. allocotantha* had
367 indeed much higher A_{net} rates than the average modeled A_{net} (Figure 4). However A_{net} from *W.*
368 *crassifolia* and *C. cretosa* were not dissimilar to the modeled values, and both these species

369 together represent 46% of the trees in the plot other, whereas *C. cuneata* and *S. allocotantha*
370 together represent ~ 5%. If the unmeasured species in the plot (~ 50 species) have photosynthetic
371 capacity similar to the latter species, rather than similar to *W. crassifolia* and *C. cretosa*, our
372 simulated GPP might be an underestimated. More specifically, a 20% higher plot average of
373 V_{cmax} and J_{max}, a plausible increase if the unmeasured species would behave like *C. cuneata* and
374 *S. allocotantha*, would translate in an underestimation of GPP of 1.7 Mg C ha^{-1} yr^{-1}.
375 Another explanation for underestimated GPP comes from the modeling of T_{leaf}.
376 Unfortunately, there are no published temperature-photosynthesis relationships for TMCF
377 species. In the SPA model, this relationship is relatively shallow compared to that used for
378 example by Sharkey and others (2007) (Supplementary information III). Given that the
379 photosynthetic parameters in the SPA model are based on measurements at T_{leaf} ~ 20 °C, and
380 average simulated T_{leaf} was around 15 °C at midday (Figure 4b), it is unlikely that the
381 temperature sensitivity of photosynthesis in SPA caused underestimations of modeled V_{cmax} and
382 J_{max} (and hence A_{net}). A more plausible explanation comes from the underestimation of modeled
383 T_{leaf} compared with field-measured values (Fig 4a and 4b). The T_{leaf} measurements between 8:00
384 and 17:00 were on average 3.25 °C higher than the modeled values between those hours, and
385 increasing modeled T_{leaf} by 3.25 °C would lead to 15.6% higher V_{cmax} and J_{max} values during the
386 day time. For annual GPP values this implies a potential underestimation of ~ 1.3 Mg C ha^{-1} yr^{-1}
387 in our original model runs. Combined, the potential underestimation of photosynthetic parameter
388 values (V_{cmax} and J_{max}) and T_{leaf} contribute up to one-third (~3.2 Mg C ha^{-1} yr^{-1}) of the 10 Mg C
389 ha^{-1} yr^{-1} discrepancy between the study from Girardin and others (2013) and this one.
390

391 The difference in GPP estimates Girardin and others (2013) and this study can
392 furthermore be explained by potential overestimates of the carbon expenditure (R_a and NPP) in
393 the former study, as this forms the basis for their GPP calculations. Girardin and others (2013)
394 indicated that their values of R_a, and consequently GPP, could be overestimated due uncertainties
395 in scaling stem respiration (R_{stem}) from woody tissue surface area data. For example, Robertson
396 and others (2010) report a stem area index (SAI) of 1.45 and a R_{stem} of 0.62 µmol m^{-2} s^{-1} from a
397 short campaign for the same site where Girardin and others (2013) give an SAI of 2.03 and R_{stem}
398 of 1.1 mmol m^{-2} s^{-1}. Using the values from Robertson and others (2010), total R_a, and hence the
399 GPP estimate, would be 5.6 Mg C ha^{-1} yr^{-1} closer to our estimate. Additionally, total R_a could be
400 overestimated by Girardin and others (2013) because all day time respiration measures of R_a
401 were scaled to average daily temperature with a Q10 of 2.0 while Q10 values, in general, are
402 higher in biomes with a lower average T_{air} (Tjoelker and others 2001). For the research site, with
403 an annual temperature of 12.5 °C, application of the decline in Q10 with temperature proposed
404 by Tjoelker and others (2001) would mean a Q10 of 2.65. If used, this would reduce R_a and
405 therefore GPP with 1.7 Mg C ha^{-1} yr^{-1}.
406 Quantifying uncertainty in the estimates from Girardin and others (2013) was beyond the
407 aims of this study. Nonetheless, both possible underestimates of the modeled GPP in this study
408 and possible overestimates in the summing of NPP and R_a can explain the discrepancy of 10 Mg
409 C ha^{-1} yr^{-1} between two GPP estimates from the same research site. The large error terms in the
410 component summation method have been acknowledged elsewhere and are currently difficult to
411 constrain (*e.g.* Malhi and others 2009, Girardin and others 2013). They offer a unique view into
412 interpreting GPP, and we note that substantial reductions would be needed for them to account in
413 isolation for the discrepancy between the two GPP estimates. Nonetheless, the use of site-

414 species- and leaf-level data in the modeling exercise we present here is unprecedented for
415 tropical montane forest physiology. Based on the GPP estimation of 16.2 Mg C ha^{-1} yr^{-1} with
416 potential underestimation of the model of 3.2 Mg C ha^{-1} yr^{-1}, it seems that the GPP of TMCFs at
417 this altitude are indeed significantly smaller than lowland rainforest by 30-40%.
418

419 **Conclusions**

420 This study presents a process-based simulated annual GPP of a TMCF, parameterized
421 with field measurements of biochemical photosynthetic capacity (V_{cmax} and J_{max}) and other
422 physical vegetation parameters. The SPA model slightly underestimated daily transpiration rates
423 when compared with *in situ* data, but simulated stomatal opening and closure correctly. In
424 contrast, measurements of A_{net} and T_{leaf} indicate a potential underestimation of photosynthesis by
425 the model. Overall, this modeling exercise confirms earlier hypotheses that (for tropical
426 ecosystems) the long-observed low NPP of TMCFs is strongly influenced by lower GPP, which
427 in turn is mostly explained by the characteristically lower T_{air} , PAR and LAI, though their
428 relative importance may alter with location and elevation. Furthermore, GPP decreases slightly
429 in the dry season (with 17%), but not as a consequence of drought stress. Our analysis indicates
430 that the GPP of our study TMCF at 3025 m a.s.l. is substantially smaller than that of lowland
431 rainforest, by 30-40% or more, and that this difference can be mostly attributed to the effect of
432 lower temperatures. The uncertainties discussed in estimating GPP highlight the challenges that
433 still exist in quantifying one of the most important fluxes in the terrestrial carbon cycle.
434

435 **Acknowledgements**

436 This study is a product of the Andes Biodiversity and Ecosystems Research Group. This study
437 was financed by a grant from the Andes-Amazon program of the Gordon and Betty Moore
438 Foundation, with research grants from the UK Natural Environment Research Council, a Royal
439 Geographical Society (with IBG) geographical fieldwork grant and a scholarship from the
440 School of Geosciences from the University of Edinburgh. We also thank the Asociación para la
441 Conservación de la Cuenca Amazónica (ACCA) for hosting us at the Wayqecha field station and
442 INRENA for permitting us to explore the Peruvian tropical forest. We thank Rob St John for
443 indispensible help with the sap flow system.
444

445 **References**

446 Adamek, M, Corre, MD, Holscher, D, 2009. Early effect of elevated nitrogen input on above-
447 ground net primary production of a lower montane rain forest, Panama. Journal of Tropical
448 Ecology 25, 637-647.

449 Bruijnzeel, LA, Veneklaas, EJ, 1998. Climatic conditions and tropical, montane forest
450 productivity: The fog has not lifted yet. Ecology 79, 3-9.

451 Čermák, J, Deml, M, Penka, M, 1973. A new method of sap flow rate determination in trees.
452 Biol Plant 15, 171-178.

453 Čermák, J, Kucera, J, Nadezhdina, N, 2004. Sap flow measurements with some thermodynamic
454 methods, flow integration within trees and scaling up from sample trees to entire forest stands.
455 Trees-Structure and Function 18, 529-546.

456 Domingues, TF, Berry, JA, Martinelli, LA, Ometto, J, Ehleringer, JR, 2005. Parameterization of
457 canopy structure and leaf-level gas exchange for an eastern Amazonian tropical rain forest
458 (tapajos national forest, para, brazil). Earth Interactions 9.

459 Farquhar, GD, Caemmerer, SV, Berry, JA, 1980. A biochemical-model of photosynthetic co2
460 assimilation in leaves of c-3 species. Planta 149, 78-90.

461 Fisher, J, Malhi, Y, Torres, I, Metcalfe, D, Weg, M, Meir, P, Silva-Espejo, J, Huasco, W, 2013.
462 Nutrient limitation in rainforests and cloud forests along a 3,000-m elevation gradient in the
463 Peruvian andes. Oecologia 172, 889-902.

464 Fisher, JB, Malhi, Y, Bonal, D, Da Rocha, HR, De AraÚJo, AC, Gamo, M, Goulden, ML,
465 Hirano, T, Huete, AR, Kondo, H, Kumagai, TO, Loescher, HW, Miller, S, Nobre, AD,
466 Nouvellon, Y, Oberbauer, SF, Panuthai, S, Roupsard, O, Saleska, S, Tanaka, K, Tanaka, N, Tu,
467 KP, Von Randow, C, 2009. The land–atmosphere water flux in the tropics. Global Change
468 Biology 15, 2694-2714.

469 Fisher, RA, Williams, M, da Costa, AL, Malhi, Y, da Costa, RF, Almeida, S, Meir, P, 2007. The
470 response of an eastern amazonian rain forest to drought stress: Results and modelling analyses
471 from a throughfall exclusion experiment. Global Change Biology 13, 2361-2378.

472 Fisher, RA, Williams, M, de Lourdes Ruivo, M, de Costa, AL, Meir, P, 2008. Evaluating
473 climatic and soil water controls on evapotranspiration at two amazonian rainforest sites.
474 Agricultural and Forest Meteorology 148, 850-861.

475 Fisher, RA, Williams, M, Do Vale, RL, Da Costa, AL, Meir, P, 2006. Evidence from amazonian
476 forests is consistent with isohydric control of leaf water potential. Plant Cell and Environment
477 29, 151-165.

478 Fox, A, Williams, M, Richardson, AD, Cameron, D, Gove, JH, Quaife, T, Ricciuto, D,
479 Reichstein, M, Tomelleri, E, Trudinger, CM, Van Wijk, MT, 2009. The reflex project:
480 Comparing different algorithms and implementations for the inversion of a terrestrial ecosystem
481 model against eddy covariance data. Agricultural and Forest Meteorology 149, 1597-1615.

482 Girardin, CAJ, Malhi, Y, AragÃO, LEOC, Mamani, M, Huaraca Huasco, W, Durand, L, Feeley,
483 KJ, Rapp, J, Silva-Espejo, JE, Silman, M, Salinas, N, Whittaker, RJ, 2010. Net primary
484 productivity allocation and cycling of carbon along a tropical forest elevational transect in the
485 peruvian andes. Global Change Biology 16, 3176-3192.

486 Girardin, CAJ et al. 2013. Productivity and carbon allocation in a tropical montane cloud forest
487 in the Peruvian Andes. Plant Ecology & Diversity. In pres.

488 Grubb, PJ, Whitmore, TC, 1966. A comparison of montane and lowland rain forest in ecuador .2.
489 Climate and its effects on distribution and physiognomy of forests. Journal of Ecology 54, 303-
490 333.

491 Hirata, R, Saigusa, N, Yamamoto, S, Ohtani, Y, Ide, R, Asanuma, J, Gamo, M, Hirano, T,
492 Kondo, H, Kosugi, Y, Li, S-G, Nakai, Y, Takagi, K, Tani, M, Wang, H, 2008. Spatial
493 distribution of carbon balance in forest ecosystems across east asia. Agricultural and Forest
494 Meteorology 148, 761-775.

Hutyra, LR, Munger, JW, Hammond-Pyle, E, Saleska, SR, Restrepo-Coupe, N, Daube, BC, de Camargo, PB, Wofsy, SC, 2008. Resolving systematic errors in estimates of net ecosystem exchange of CO_2 and ecosystem respiration in a tropical forest biome. Agricultural and Forest Meteorology 148, 1266-1279.

Kaimal, JC, Finnigan, JJ, 1994. Atmospheric boundary layer flows : Their structure and measurement. Oxford University Press, New York ; Oxford.

Kitayama, K, Aiba, SI, 2002. Ecosystem structure and productivity of tropical rain forests along altitudinal gradients with contrasting soil phosphorus pools on mount kinabalu, borneo. Journal of Ecology 90, 37-51.

Lemmon PE. 1956. A spherical densiometer for estimating forest overstory density. Forest Sci 2:314-320.

Letts, MG, Mulligan, M, 2005. The impact of light quality and leaf wetness on photosynthesis in north-west andean tropical montane cloud forest. Journal of Tropical Ecology 21, 549-557.

Malhi, Y, Aragao, L, Metcalfe, DB, Paiva, R, Quesada, CA, Almeida, S, Anderson, L, Brando, P, Chambers, JQ, da Costa, ACL, Hutyra, LR, Oliveira, P, Patino, S, Pyle, EH, Robertson, AL, Teixeira, LM, 2009. Comprehensive assessment of carbon productivity, allocation and storage in three Amazonian forests. Global Change Biology 15, 1255-1274.

Marthews, TR, Malhi, Y, Girardin, CAJ, Silva Espejo, JE, Aragão, LEOC, Metcalfe, DB, Rapp, JM, Mercado, LM, Fisher, RA, Galbraith, DR, Fisher, JB, Salinas-Revilla, N, Friend, AD, Restrepo-Coupe, N, Williams, RJ, 2012. Simulating forest productivity along a neotropical

515 elevational transect: Temperature variation and carbon use efficiency. Global Change Biology
516 18, 2882-2898.

517 McMurtrie, RE, Comins, HN, Kirschbaum, MUF, Wang, YP, 1992. Modifying existing forest
518 growth models to take account of effects of elevated CO_2. Australian Journal of Botany, 40, 657-
519 677.

520 Meir P, Kruijt B, Broadmeadow M., Kull O, Carswell F, Nobre A & Jarvis PG (2002).
521 Acclimation of photosynthetic capacity to irradiance in tree canopies in relation to leaf nitrogen
522 concentration and leaf mass per unit area. *Plant Cell and Environment*, 25, 343-357.

523 Moser, G, Hertel, D, Leuschner, C, 2007. Altitudinal change in lai and stand leaf biomass in
524 tropical montane forests: A transect shady in Ecuador and a pan-tropical meta-analysis.
525 Ecosystems 10, 924-935.

526 Raich, JW, Russell, AE, Vitousek, PM, 1997. Primary productivity and ecosystem development
527 along an elevational gradient on mauna loa, hawai‘i. Ecology 78, 707-721.

528 Santiago, LS, Goldstein, G, Meinzer, FC, Fownes, JH, Mueller-Dombois, D, 2000. Transpiration
529 and forest structure in relation to soil waterlogging in a Hawaiian montane cloud forest. Tree
530 Physiology 20, 673-681.

531 Saxton, KE, Rawls, WJ, Romberger, JS, Papendick, RI, 1986. Estimating generalized soil-water
532 characteristics from texture. Soil Sci Soc Am J 50, 1031-1036.

533 Sharkey, TD, Bernacchi, CJ, Farquhar, GD, Singsaas, EL, 2007. Fitting photosynthetic carbon
534 dioxide response curves for C-3 leaves. Plant Cell and Environment 30, 1035-1040.

535 Tanner, EVJ, Kapos, V, Franco, W, 1992. Nitrogen and phosphorus fertilization effects on
536 venezuelan montane forest trunk growth and litterfall. Ecology 73, 78-86.

537 Tanner, EVJ, Kapos, V, Freskos, S, Healey, JR, Theobald, AM, 1990. Nitrogen and phosphorus
538 fertilization of Jamaican montane forest trees. Journal of Tropical Ecology 6, 231-238.

539 Tanner, EVJ, Vitousek, PM, Cuevas, E, 1998. Experimental investigation of nutrient limitation
540 of forest growth on wet tropical mountains. Ecology 79, 10-22.

541 van de Weg, MJ, Meir, P, Grace, J, Atkin, OK, 2009. Altitudinal variation in leaf mass per unit
542 area, leaf tissue density and foliar nitrogen and phosphorus content along an Amazon-Andes
543 gradient in Peru. Plant Ecology & Diversity 2, 243-254.

544 van de Weg, MJ, Meir, P, Grace, J, Damian Ramos, G, 2012. Photosynthetic parameters, dark
545 respiration and leaf traits in the canopy of a Peruvian tropical montane cloud forest. Oecologia
546 168, 23-34.

547 Vitousek, P, Farrington, H, 1997. Nutrient limitation and soil development: Experimental test of
548 a biogeochemical theory. Biogeochemistry 37, 63-75.

549 Waide, RB, Zimmerman, JK, Scatena, FN, 1998. Controls of primary productivity: Lessons from
550 the luquillo mountains in Puerto Rico. Ecology 79, 31-37.

551 Wang, HQ, Hall, CAS, Scatena, FN, Fetcher, N, Wu, W, 2003. Modeling the spatial and
552 temporal variability in climate and primary productivity across the Luquillo Mountains, Puerto
553 Rico. Forest Ecology and Management 179, 69-94.

554 Williams, M, Law, BE, Anthoni, PM, Unsworth, MH, 2001a. Use of a simulation model and
555 ecosystem flux data to examine carbon-water interactions in ponderosa pine. Tree Physiology 21.

556 Williams, M, Malhi, Y, Nobre, AD, Rastetter, EB, Grace, J, Pereira, MGP, 1998. Seasonal
557 variation in net carbon exchange and evapotranspiration in a Brazilian rain forest: A modelling
558 analysis. Plant Cell and Environment 21, 953-968.

559 Williams, M, Rastetter, EB, Fernandes, DN, Goulden, ML, Wofsy, SC, Shaver, GR, Melillo, JM,
560 Munger, JW, Fan, SM, Nadelhoffer, KJ, 1996. Modelling the soil-plant-atmosphere continuum
561 in a quercus-acer stand at harvard forest: The regulation of stomatal conductance by light,
562 nitrogen and soil/plant hydraulic properties. Plant, Cell & Environment 19, 911-927.

563 Williams, M, Rastetter, EB, Shaver, GR, Hobbie, JE, Carpino, E, Kwiatkowski, BL, 2001b.
564 Primary production of an arctic watershed: An uncertainty analysis. Ecological Applications 11,
565 1800-1816.

566 Wright, JK, Williams, M, Starr, G, McGee, J, Mitchell, RJ, 2013. Measured and modelled leaf
567 and stand-scale productivity across a soil moisture gradient and a severe drought. Plant, Cell &
568 Environment 36, 467-483.

569 Wullschleger, SD, 1993. Biochemical limitations to carbon assimilation in c3 plants—a
570 retrospective analysis of the A/C_i curves from 109 species. J Exp Bot 44, 907-920.

571 Zimmermann M, Meir P, Bird MI, Malhi Y, Ccahuana AJQ. 2009. Climate dependence of
572 heterotrophic soil respiration from a soil-translocation experiment along a 3000 m tropical forest
573 altitudinal gradient. European Journal of Soil Science 60:895-906.

574 Zimmermann M, Meir P, Silman MR, Fedders A, Gibbon A, Malhi Y, Urrego DH, Bush MB,
575 Feeley KJ, Garcia KC, Dargie GC, Farfan WR, Goetz BP, Johnson WT, Kline KM, Modi AT,
576 Rurau NMQ, Staudt BT, Zamora F. 2010. No differences in soil carbon stocks across the tree
577 line in the Peruvian Andes. Ecosystems 13: 62-74.

578 Zotz G, Tyree MT, S. Patino S, Carlton MR. 1998. Hydraulic architecture and water use of
579 selected species from a lower montane forest in Panama. Trees-Structure and Function 12:302-
580 309.
581

582 Tables

583 Table 1. Photosynthetic parameters V_{cmax} and J_{max} per canopy layer and proportion of leaves per canopy layer as

584 represented in a standard run of the SPA model.

Canopy layer (1= top canopy)	V_{cmax} **(μmol m^{-2} s^{-1})**	J_{max} **(μmol m^{-2} s^{-1})**	**Proportion of leaves per layer**
1	45.9	95.2	0.203
2	34.6	81.2	0.350
3	28.3	62.5	0.214
4	23.2	50.9	0.143
6	12.8	29.1	0.052
7	15.4	30.6	0.017
8	15.1	29.9	0.011
9	0	0	0
10	0	0	0

585
586

587 Table 2. Structural parameters and their units used in the standard SPA model simulations and their origins.

588

Parameter	Units	Value	Source
Canopy height	m	12.8	Field observations
Aboveground conductance	m^2 MPa $mmol^{-1}$	3.5	Parameterised according to leaf specific conductivity (*LSC*)
Root resistivity	MPa s g $mmol^{-1}$	140	Parameterised according to leaf specific conductivity (*LSC*)
Rooting depth	m	0.3	Field observations
Iota	dimensionless	0.0007	Set
Capacitance	mmol MPa^{-1} m^{-2}	5000	Set

589 Table 3. Units and standard values for the average parameters used in the SPA model, and their maximum and
590 minimum values as measured in the field and used in the sensitivity analyses. The parameters are listed from top to
591 bottom or which **Δ**GPP, the absolute change in GPP between model runs with minimum and maximum parameter
592 values, was highest. Relative sensitivity per parameter of driver was calculated by dividing the % change in
593 parameter or driver from minimum to maximum observed by the % change in simulated GPP. When **Δ**GPP was 0,
594 no value for the ratio of change could be calculated.

Factor	**Unit**	**standard**	**maximum**	**minimum**	**ΔGPP (Mg C ha^{-1} yr^{-1})**	**Ratio of change**
Daily PAR	mol m^{-2} d^{-1}	20.1	43.2	4.0	14.7	0.24
V_{cmax} / J_{max}	µmol m^{-2} s^{-1}	46 / 95	93.9 / 140	14.9 / 26	14.3	0.46
Daily SWR	MJ m^{-2} d^{-1}	8.765	20.3	1.76	12.7	0.22
LAI (N in leaves stays constant)	m^{-2}m^{-2}	4.17	5.6	2.6	6.7	0.59
Daily temperature	ºC	10.44	13.26	7.34	3.8	0.35
Fraction diffuse light	-	0.42	1	0.2	2.8	0.09
LAI (N in canopy constant)	m^{-2}m^{-2}	4.17	5.6	2.6	0.42	0.03
Daily VPD kPa	kPa	0.14	0.36	0.03	-0.05	-0.01
Total root biomass m^{-2}	G	3291	5420	1967	-	-
Root resistivity	MPa s g mmol^{-1}	145	180	120	-	-
Plant conductivity	mmol m^{-1} s^{-1} MPa^{-1}	3.5	4.4	2.75	-	-
Soil water content	m^{-3}m^{-3}	0.29	0.367	0.196	-	-
Iota (ι)	dimensionless	0.0007	0.001	0.0001	-	-
Capacitance	mmol m^{-2} LA	5000	3000	7000	-	-

MPa^{-1}

595

Table 4. The factors used to simulate TMCF under typical lowlands tropical rainforests conditions, as well as the simulated GPP and % in increase compared to a standard run of the SPA model (GPP = 16.24 Mg C ha^{-1} yr^{-1}).

Factor	**Unit**	**Value**	**Simulated GPP (Mg C ha^{-1} yr^{-1})**	**% Increase in GPP**
T_{air}	°C	26	21.2 ± 2.1	30.3
LAI	$m^{-2}m^{-2}$	5.5	19.0 ± 1.9	17.2
PAR	mol m^{-2} d^{-1}	24.2	18.6 ± 1.9	14.9
T_{air} + PAR + LAI		all above	28.3 ± 2.8	74.9

600 Figures

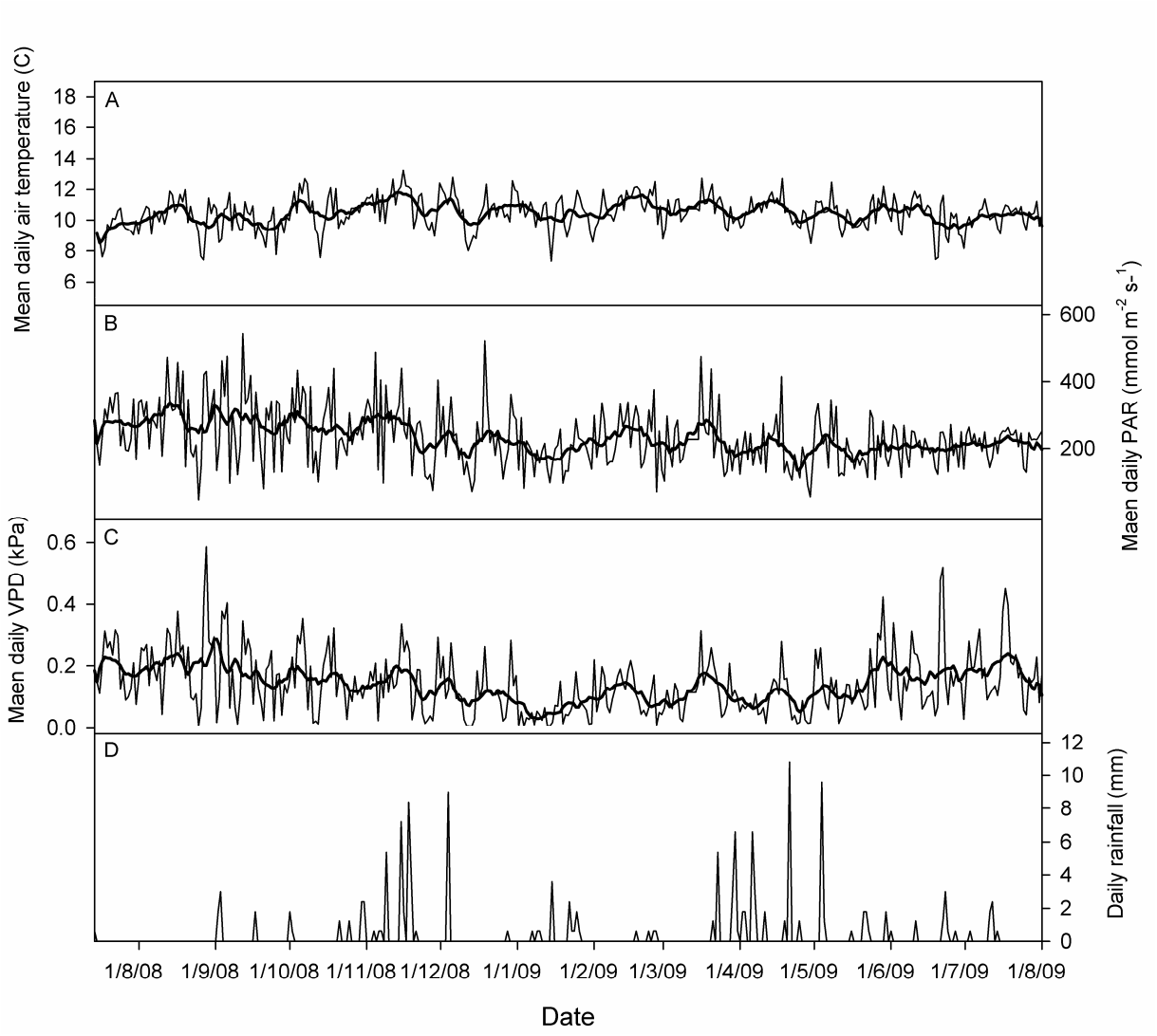

601

602

603

604 Figure 1. Meteorological variables as measured at the research site and used for driving the standard run of the SPA
605 model for the period between 14 July January 2008 and 13 July 2009 and their 10 daily average values (thick line).
606 a) mean daily temperature, b) mean daily photosynthetically active radiation (PAR), c) mean daily vapour pressure
607 deficit (VPD), and d) total daily rainfall.

608

609

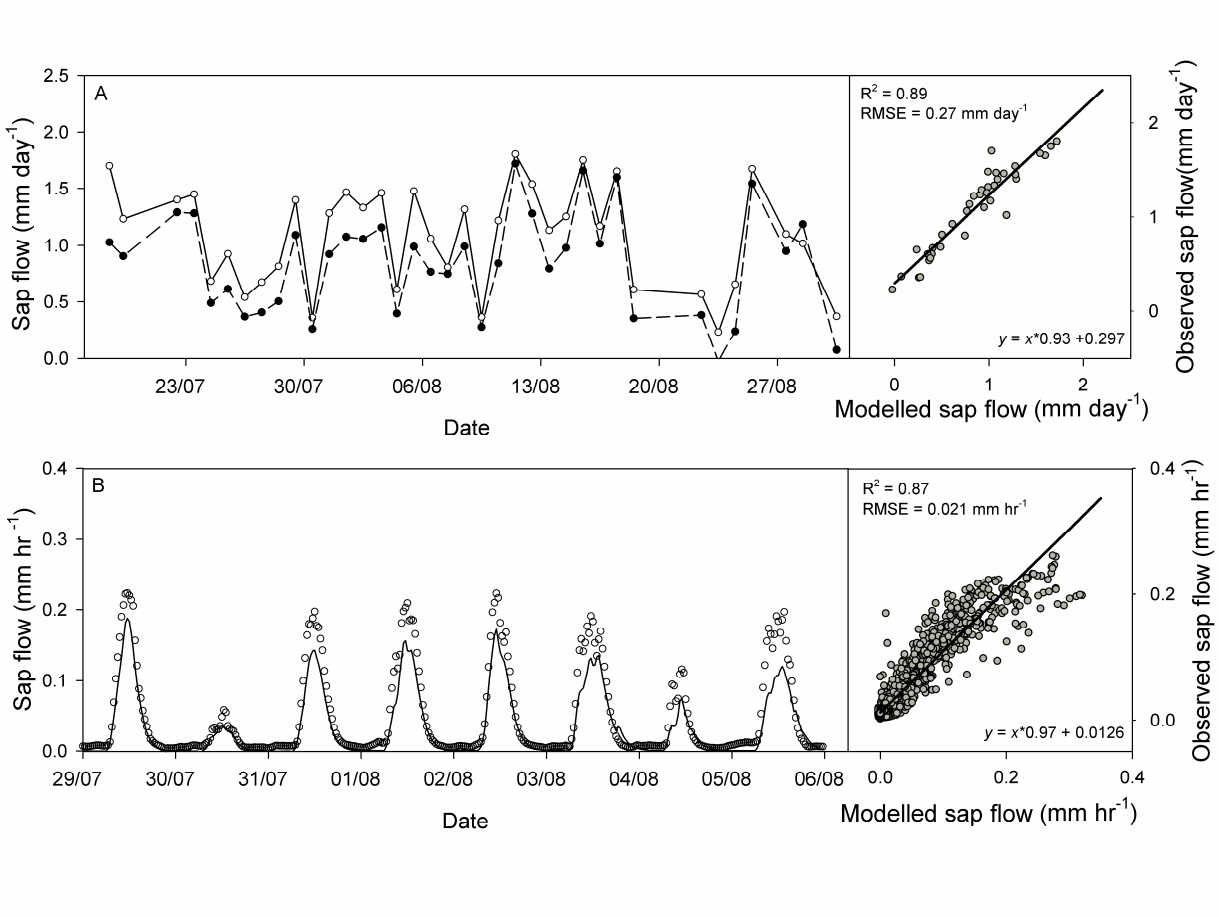

610

611

612 **Figure 2.** A) Simulated (black circles) and observed (open circles) stand-scale daily sap flow for the period from 18
613 July 2008 to 31 August 2008. B) Hourly sap flow (open circles) together with the modelled values (line) during one
614 representative week from the period displayed in graph A. Both right panes show the modelled and observed sap
615 flow values for the whole period July 2008 to 31 August 2008. Dotted lines represent 1:1 lines

616

617

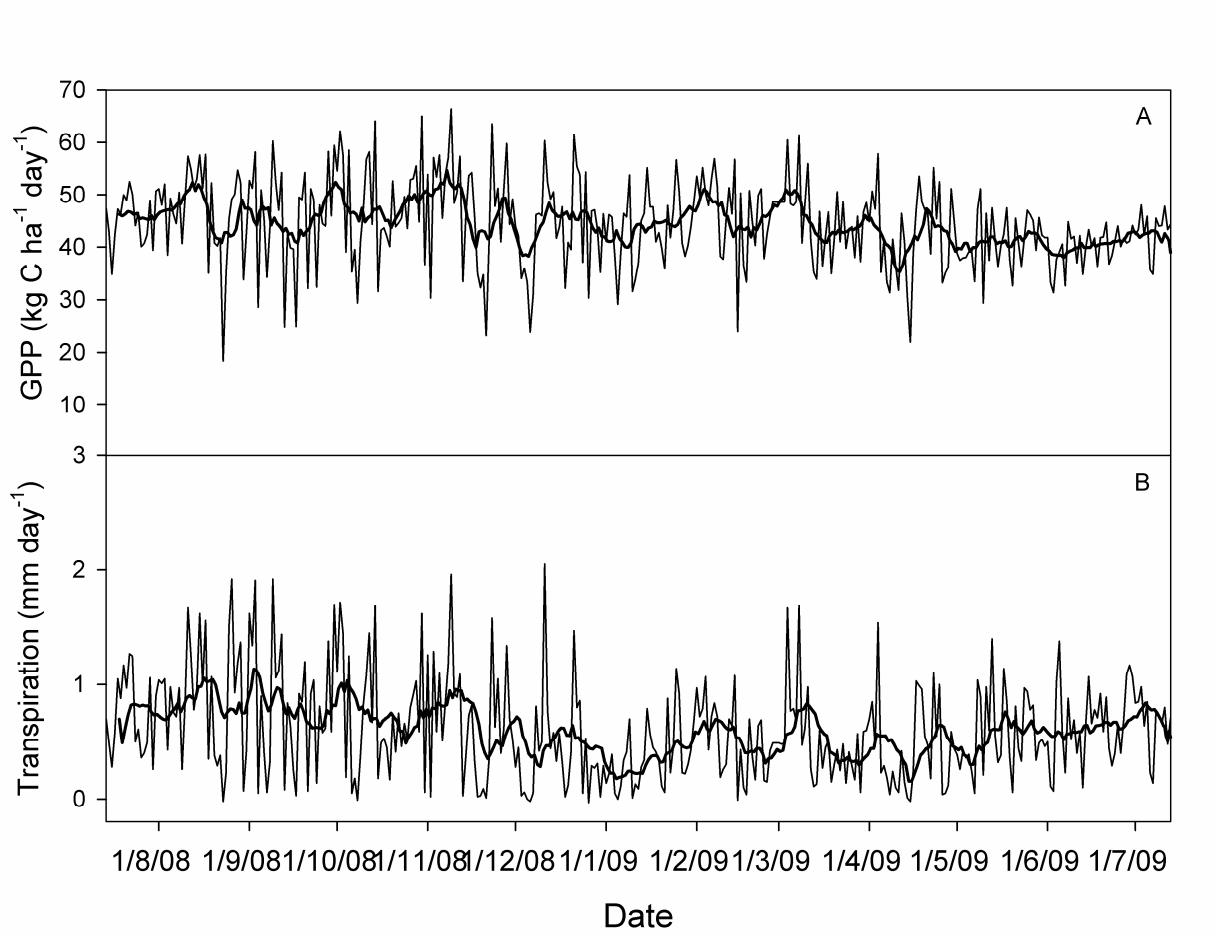

618

619 Figure 3. Simulated daily GPP (a) and transpiration (b), resulting from the standard input in the SPA model from 14

620 July 2008 to 13 July 2009. The thick lines represent a plot of data averaged as a 10-day running mean.

621

622 Figure 4

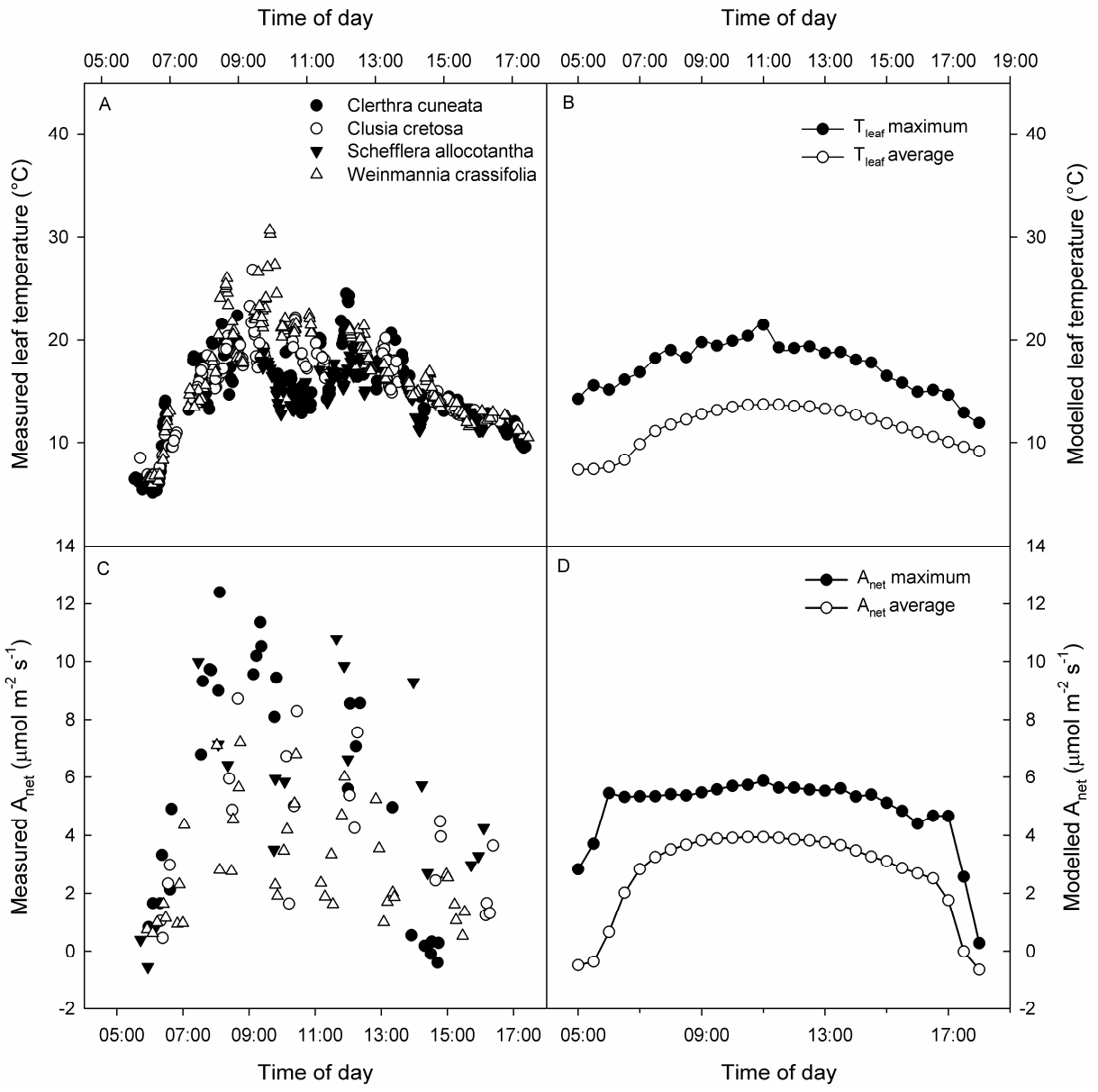

623

624 Figure 4. Diurnal measurements and modelled values of fully sun-lit full grown leaves for T_{leaf} (a and b) and A_{net} (c

625 and d). The measured values originate from the four abundant species measured in July and August 2008 .

626

627

628

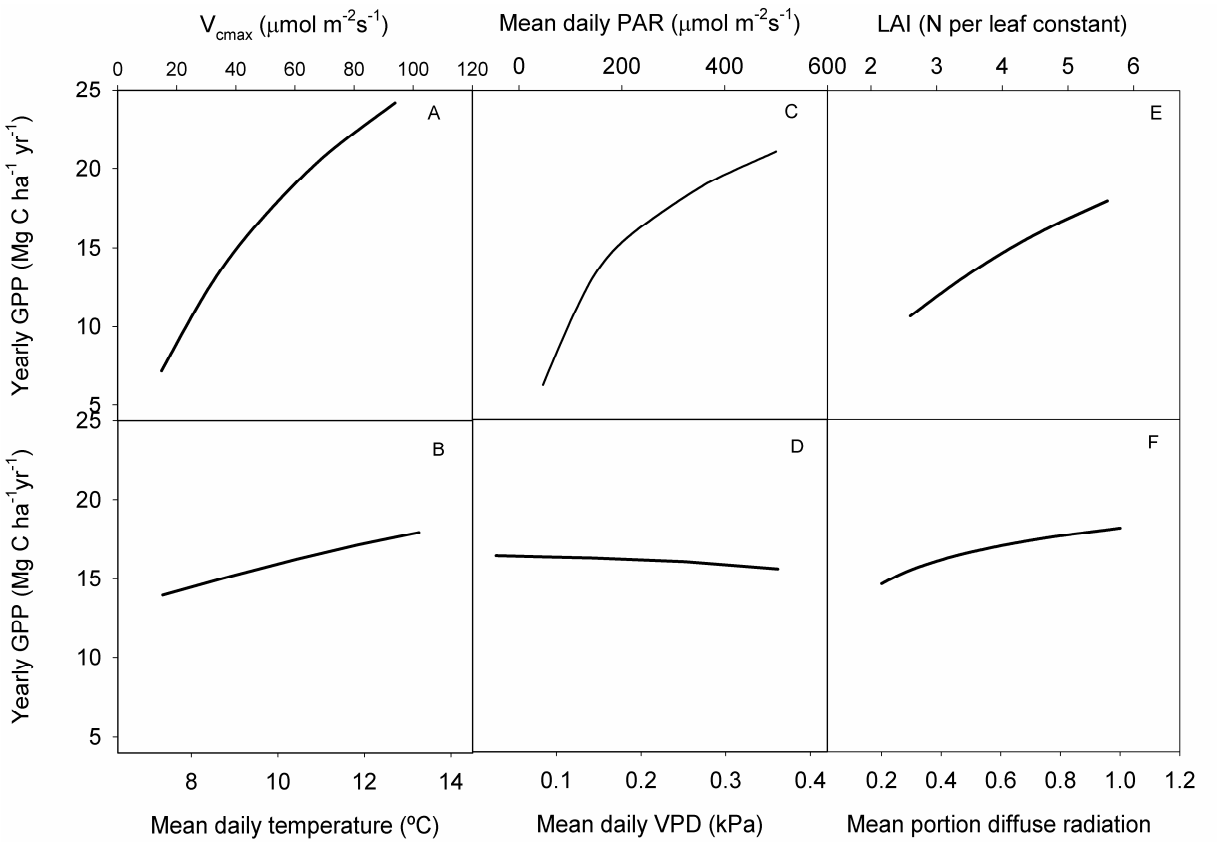

629

630 Figure 5. Results from the one-dimensional sensitivity analyses for six important factors over their observed range

631 controlling annual TMCF GPP. Note that for panel A, both V_{cmax} and J_{max} were changed concurrently, while only

632 $V_{cmax,}$ and only the value of the top layer of the canopy is listed on the X-axis.

633

634